

# Harnessing Tunable Scanning Probe Techniques to Measure Shear Enhanced Adhesion of Gecko-Inspired Fibrillar Arrays

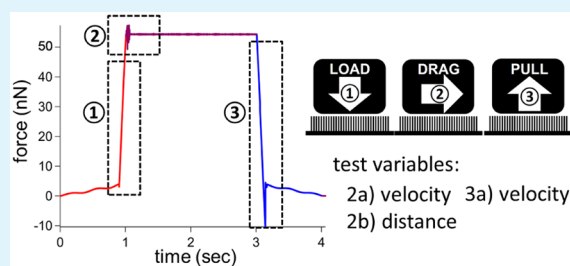
Yasong Li,<sup>†</sup> James H.-W. Zhou,<sup>§</sup> Cheng Zhang,<sup>‡</sup> Carlo Menon,<sup>†</sup> and Byron D. Gates<sup>\*,§</sup>

<sup>†</sup>Menrva Lab, School of Engineering Science, <sup>‡</sup>School of Engineering Science, and <sup>§</sup>Department of Chemistry and 4D LABS, Simon Fraser University, 8888 University Drive, Burnaby, British Columbia V5A 1S6, Canada

## Supporting Information

**ABSTRACT:** The hierarchical arrays of mesoscale to nanoscale fibrillar structures on a gecko's foot enable the animal to climb surfaces of varying roughness. Adhesion force between the fibrillar structures and various surfaces is maximized after the gecko drags its foot in one direction, which has also been demonstrated to improve the adhesion forces of artificial fibrillar arrays. Essential conditions that influence the magnitude of these interactions include the lateral distance traveled and velocity between the contacting surfaces, as well as the velocity at which the two surfaces are subsequently separated. These parameters have, however, not been systematically investigated to assess the adhesion properties of artificial adhesives. We introduce a systematic study that investigates these conditions using a scanning probe microscope to measure the adhesion forces of artificial adhesives through a process that mimics the mechanism by which a gecko climbs. The measured adhesion response was different for arrays of shorter and longer fibrils. These results from 9000 independent measurements also provide further insight into the dynamics of the interactions between fibrillar arrays and contacting surfaces. These studies establish scanning probe microscopy techniques as a versatile approach for measuring a variety of adhesion properties of artificial fibrillar adhesives.

**KEYWORDS:** adhesion forces, dry adhesive, nanostructured fibrils, scanning probe microscopy, shear loading



## 1. INTRODUCTION

Geckos can maneuver themselves freely on various surfaces, irrespective of gravity, thanks to millions of nanosize fibrils on their climbing feet.<sup>1</sup> Numerous intermolecular forces collectively form a strong adhesion through contact between these slender fibrils and the surfaces upon which the gecko is climbing. The hierarchical fibrillar structures on the gecko's feet have a critical dimension in the range from micrometers to nanometers that provide both a compliancy and stickiness with the climbing surfaces.<sup>2</sup> The bonds formed between the nanofibrils and the contacting surfaces reach their strongest values after the gecko applies a lateral dragging movement of the foot toward their body.<sup>3</sup> This dragging movement has been proven to assist in the fibril alignment with the surfaces, increasing the contacting area of the interfaces and, hence, improving the adhesion forces measured in subsequent pull up experiments.<sup>4,5</sup> Test procedures that include this dragging movement have been named the "load–drag–pull" (LDP) method.<sup>6</sup> This method can be described in the following three steps: (i) the fibrillar patch first vertically approaches the contacting surfaces; (ii) a lateral shear force is applied in one direction to the patch upon contact with the surfaces; and (iii) a vertical withdrawing force is applied to the patch until the two interfaces have been completely separated. This test procedure has been performed for the analysis of gecko adhesives<sup>7,8</sup> and artificial fibrillar adhesives.<sup>9–11</sup> Results of these studies generally demonstrated an increase of adhesion measured using the LDP

method in contrast to methods without the dragging movement. These results further support the hypothesis that fibrils are aligning during the dragging process. Alignment of the fibrils could optimize the contact area during these LDP-based adhesion force measurements.

Geckos have developed certain patterns to efficiently climb. Autumn et al.<sup>12</sup> investigated the dynamics of a living gecko while climbing vertically at different speeds. Geckos generally use a stable stride pattern no matter how fast they climb, indicating that there should be an optimal set of attaching and detaching parameters that the gecko uses for efficient climbing. Artificial fibrillar adhesives are designed to mimic the geometry of the gecko fibrillar adhesives, yet can have a significant variation in their shapes, sizes and average surface coverage depending on the different preparation methods.<sup>13–16</sup> There will also be an optimal set of parameters to efficiently utilize each specific type of artificial adhesive. The LDP characterization method described above could be adapted as a technique to identify an optimal set of operating parameters for artificial fibrillar adhesives. The outcome of this study would be beneficial to applications involving these artificial adhesives, such as climbing robots,<sup>17</sup> surgical tapes,<sup>18</sup> and tools to handle microelectronic chips.<sup>19</sup>

Received: September 30, 2014

Accepted: December 30, 2014

Published: December 30, 2014



The LDP technique for measuring adhesion forces involves a dynamic interaction of the contacting interface. These dynamics can be characterized by the lateral distance and velocity of movement between the contacting surfaces and the velocity at which the two surfaces are subsequently separated. In addition to measuring adhesion forces, frictional forces are one of the most investigated properties using the LDP method.<sup>9–11,20–22</sup> Studies by Gravish et al.<sup>23</sup> demonstrated a different friction and adhesion response of gecko setae and synthetic fibrillar adhesive while varying the lateral drag velocities during LDP based measurements. Puthoff et al.<sup>24</sup> also provided evidence of the effects of drag distance and drag velocity on the adhesion and friction of fibrillar adhesives measured using LDP methods. The work of Gravish et al. and Puthoff et al. reach similar conclusions on the adhesion behavior for synthetic dry adhesives. The drag distance and velocity were, generally, directly proportional to the measured adhesion and friction forces when studying gecko setae. The result from the analysis of artificial fibrillar adhesives indicated that the adhesion and friction response both reach a point of saturation at a certain combination of drag distance and velocity. Each of these studies used relatively large areas for the analysis of each sample. For example, an analysis would use an entire gecko seta and an artificial adhesive of a similar size (e.g.,  $\sim 5 \text{ mm}^2$ ).<sup>24</sup>

A technique developed in our laboratory demonstrated the utility of a scanning probe microscope (SPM) to characterize the uniformity and adhesion properties of fibrillar arrays.<sup>5,25</sup> This technique enabled the automatic collection of data on adhesion response and the ability to observe the interactions between two contacting substances for a smaller number of fibrils (i.e., smaller contact area). Experimental results indicated that adhesion forces were randomly distributed across fibrillar arrays, even for those that are spatially distributed in a uniform manner. This phenomenon indicated that each measurement could produce a unique result even though the test conditions were almost identical. This SPM based technique provides flexibility to conduct measurements either with or without the inclusion of a lateral motion. Various parameters that control the movement of the two contacting surfaces are tunable for each measurement, within the limitations of the SPM system.

In this study, we investigated the influence of lateral drag distance, drag velocity, and the velocity at which two substrates are separated during LDP measurements used to characterize an artificial fibrillar adhesive. Adhesion forces between arrays of polymeric fibrils and a flat atomic force microscope cantilever were measured utilizing the SPM techniques described above. These techniques offer the flexibility of independently controlling each of the measurement parameters. The lateral drag distance, drag velocity, and cantilever retract velocity were each individually studied to assess their influence on the measured adhesion forces. Statistical analysis was performed on the large data sets collected under the same test conditions at different locations within each sample. These results revealed an optimal set of parameters necessary to obtain the desirable performance of the artificial fibrillar adhesive. These optimal parameters are potentially useful for various applications requiring a quick attachment and release mechanism.

## 2. RESULTS AND DISCUSSION

In our previous study, we introduced a comparison of two methods to characterize adhesion forces between surfaces through the use of a SPM system.<sup>5</sup> One of these methods,

referred to as a Push–Pull (PP) method, manipulates an SPM controlled cantilever to vertically approach an array of fibrillar nanostructured surfaces until these opposing contacting surfaces are in intimate contact. The cantilever is subsequently withdrawn in a vertical motion until completely separating the two substrates. The second method, referred to as the Load–Drag–Pull (LDP) method, introduces an additional movement of the cantilever between the other two movements used in the PP method. During this new step, the cantilever moves horizontally (i.e., applies a shear force) across the fibrillar arrays after the two substrates were brought into contact during the preloading of the compression force. A vertical retraction or pull up of the cantilever follows this drag movement of the cantilever. The schematics in Figure 1 depict the differences

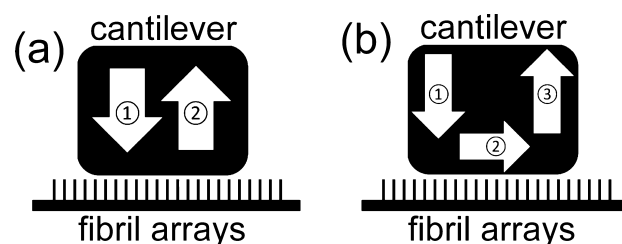


**Figure 1.** Schematic depiction of two methods used to measure adhesion forces of nanoscale fibrillar arrays: (a) the push–pull (PP) method, and (b) the load–drag–pull (LDP) method. The PP method is implemented by manipulating a scanning probe microscope (SPM) controlled tipless cantilever to vertically approach the fibrillar arrays (step 1) until the interaction force between the two surfaces reaches a preset value. The cantilever is subsequently withdrawn from the fibrillar arrays in a vertical motion (step 2) until achieving separation between the fibrils and the cantilever. The LDP method includes an additional step (see step 2 in b) between two identical steps to those of the PP method. In this additional step, the cantilever is dragged in a lateral motion over the surfaces of the fibrillar arrays to enhance fibril–cantilever interactions.

between the two methods. (Note that the actual shape of the cantilevers used in these studies is illustrated in Figure 2.) The maximum deflection of the cantilever is converted into force based on a pretest calibration of the cantilever spring constant. The force measured upon cantilever retraction is the adhesion force recorded as a single data point in the data sets used for statistical analysis. The use of an SPM system to incorporate the shear dragging movement proved to be an effective method for enhancing the adhesion force between a flat cantilever and the fibrillar arrays, which is similar to the method used by the biological adhesion system (e.g., gecko). As indicated from the existing research,<sup>12</sup> geckos use a relatively stable process of gripping and releasing surfaces regardless of their climbing speed for a given gait. The animal generally increases stride length, which is the distance between two steps, instead of changing the stride frequency, leg phase (sequences of movements within one step), and/or attachment/detachment time (intervals of the interaction between the feet and the contact surfaces until forming/breaking complete contact).<sup>12</sup> These experimental results suggest that there should be an optimal set of parameters that the animals use to create a firm grip with the climbing surfaces. The complete set of optimal parameters has not yet been confirmed with living animals. The rate-dependent adhesion force during the attachment process has been proven using separated gecko setae and artificial microscale dry adhesives, but the results provide no specific

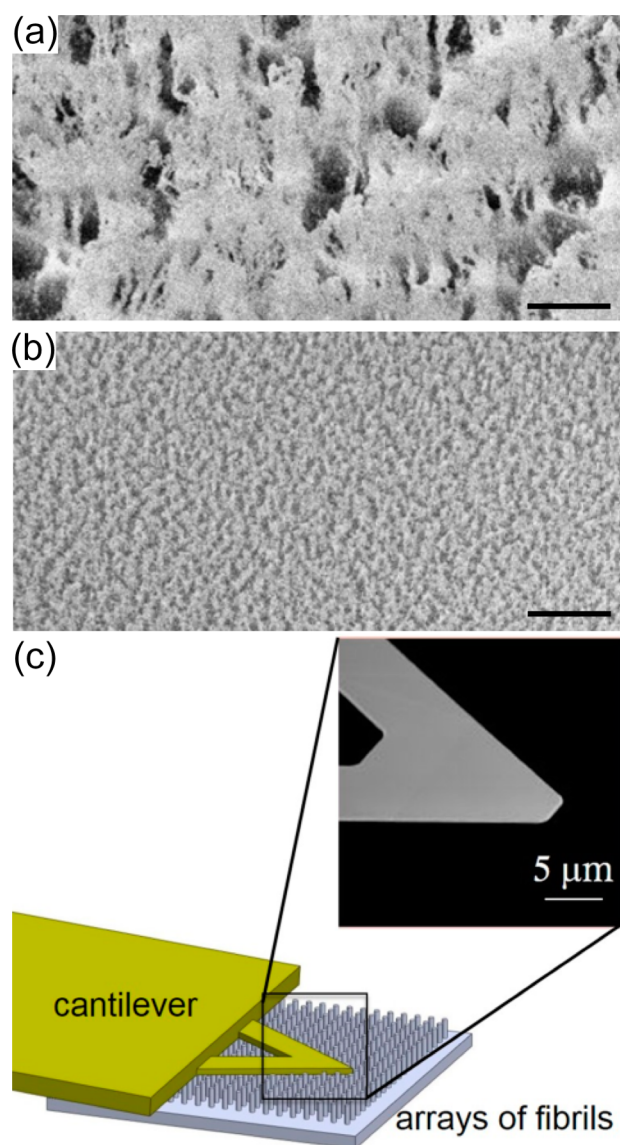


**Figure 2.** Scanning electron microscopy (SEM) images corresponding to arrays of fibrils with average heights of either (a)  $\sim 1 \mu\text{m}$  or (b)  $\sim 0.1 \mu\text{m}$ . Scale bars indicated on the SEM images represent a distance of  $2 \mu\text{m}$ . (c) Schematic depiction of the experimental setup along with an optical microscope image (inset) of a typical flat cantilever used in these studies.

optimal set of parameters.<sup>12,23,24</sup> Considering the actual size of the fibrillar structure in the biological system and in many artificial fibrillary adhesives, the SPM measurement system that we adapted for measuring nanoscale fibrillar arrays would be a suitable platform to provide further insight into a set of optimal parameters. Based on the dynamics taking place during contact between two surfaces, the force describing this interaction is related to the derivative of velocity and the second derivative of distance. Controlling the velocity and displacement of a substrate under test can, therefore, modify its interactions with an array of fibrils. Thus, three parameters that are of specific interest for further investigation include the drag distance (the relative displacement of two substrates in a lateral direction during the process of “drag”), the drag velocity (the relative velocity of two substrates in a lateral direction during the process of “drag”) and the retract velocity (the relative

velocity of two substrates in a vertical direction during the process of “pull”).

Two types of fibrillar samples were prepared (see Experimental Section for details of the preparation methods) and their adhesion forces measured using different sets of parameters. These fibrillar samples contain arrays of upright fibrils with average lengths of either  $\sim 1 \mu\text{m}$  (hereafter referred to as the longer fibrillar sample) or  $\sim 0.1 \mu\text{m}$  (hereafter referred to as the shorter fibrillar sample). These differences in aspect ratio of the longer and shorter fibrillar samples can be observed by scanning electron microscopy (Figure 2). The cantilever used in the adhesion force measurements was featureless or flat on both sides of the cantilever (Figure 2c), and would contact multiple fibrils within either type of sample during these measurements. The identical preloading conditions used in all the experiments enabled us to estimate the area of contact between the flat cantilever and these arrays (i.e., the contact area), which was  $\sim 18.7 \mu\text{m}^2$  for samples containing the longer fibrils and  $\sim 0.762 \mu\text{m}^2$  for the arrays of shorter fibrils. These estimates were based on a theoretical contact area determined from the angled approach of the flat cantilever to each of these arrays of fibrils (see the Supporting Information for further details).

**2.1. Investigation of the Drag Distance in LDP Experiments.** The optimal drag distance should provide insight into the point at which a system achieves maximum alignment of the fibrils. Excessive drag applied to the fibrils during the initial movement of the flat cantilever will reduce the initial benefits of the dragging movement, which might result from the stick–slip effect.<sup>25</sup> The stick–slip effect introduces an instability to the established points of contact. Excessive dragging movement could also increase the likelihood of fibril damage.<sup>27,28</sup> The process of the fibril alignment can be observed from the force–time (FT) curve, such that the one shown in Figure 3 that was obtained using an artificial fibrillar adhesive (see Experimental Section for further details). This FT curve depicts the interaction force measured over the time elapsed during the contact between the cantilever and fibrillar surfaces for one measurement cycle. In Figure 3, the cantilever started at a position of noncontact (showing no interaction force in the beginning of the curve), and the cantilever was brought into contact with the fibrillar arrays until the compression/preloading force reaches a preset value (compression forces are indicated by a positive value). The cantilever was subsequently dragged over a specific distance, which was varied as a test parameter (insets in Figure 3), at a dragging speed of  $20 \mu\text{m/s}$ . The cycle ended with a 2 s dwell time, followed by a vertical retraction of the cantilever to separate the surfaces as indicated by the negative force in the curve. The lowest value in the force curve was recorded as the adhesion force for a single measurement.

The measured force oscillated as the cantilever was dragged across the fibrillar surfaces, as indicated in the insets of Figure 3. The maximum range of these oscillations was  $\sim 5 \text{ nN}$ , which corresponded to a variable contact between the cantilever and the roughened surfaces. The time period over which the oscillation occurred was proportional to the dragging distance. During this lateral shear, the positive “spikes” in the force curve were attributed to the cantilever encountering an array of newly contacted fibrils. The initial interactive force is restored when the cantilever continues moving over an array of aligned fibrils. When a sufficient number of these fibrils release from the cantilever, a retraction force is measured as indicated by the

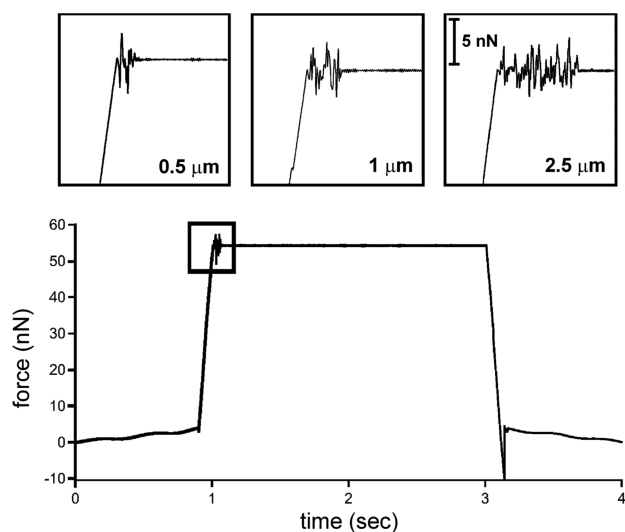


**Figure 3.** Representative force–time (FT) curve (bottom) measured using the LDP method for a cantilever in contact with an array of fibrils (in this example the fibrils had an average height of  $\sim 0.1 \mu\text{m}$ ). Drag velocity was set to  $20 \mu\text{m/s}$ . The magnified views of FT curves (from the region denoted by the black box) depict the force response corresponding to different drag distances (e.g.,  $0.5$ ,  $1.0$ , and  $2.5 \mu\text{m}$ , respectively). The length of time over which the measured forces oscillate corresponds to the distance (and thus the period of time) the cantilever is moved across the fibrillar arrays. The range of the oscillations in force during this drag step of the LDP method is  $\sim 5 \text{ nN}$ .

negative “spikes” in the force curve. A similar effect was observed in the FT curves for both the longer ( $\sim 1 \mu\text{m}$ ) and shorter ( $\sim 0.1 \mu\text{m}$ ) fibrils. Figure 3 only demonstrates the FT curves for the shorter fibrils.

The effect of drag distance on the measured adhesion force was statistically analyzed for the samples consisting of longer ( $\sim 1 \mu\text{m}$ ) and shorter ( $\sim 0.1 \mu\text{m}$ ) fibrils. The drag and retract velocities were maintained at  $20 \mu\text{m/s}$  and  $1 \mu\text{m/s}$ , respectively, whereas 400 measurements were obtained for each of the different drag distances ( $0.5$ ,  $1$ , and  $2.5 \mu\text{m}$ ). The ratio of drag distance to fibril length (referred to as the distance-to-length

ratio, or DL ratio) for the sample of shorter fibrils was  $5$ ,  $10$  and  $25$ , while the DL ratio for the sample of longer fibrils was  $0.5$ ,  $1$ , and  $2.5$ . The results of measurements performed using the PP method are also included for comparison. Figure 4a, b contains histograms for the measurements obtained from samples with fibril lengths of  $\sim 0.1 \mu\text{m}$  and  $\sim 1 \mu\text{m}$ , respectively. For the shorter fibrils ( $\sim 0.1 \mu\text{m}$ ), the longer drag distances resulted in a smaller adhesion force. In contrast, the longer fibrils (heights of  $\sim 1 \mu\text{m}$ ) displayed higher average adhesion forces for the longer drag distances. Considering the DL ratio and the median or trimmed mean of the adhesion measurements, the tests at a DL ratio of  $5$  for the sample of shorter fibrils gave a similar result to that from the PP method. However, the results of tests at a DL ratio of  $2.5$  for the sample of longer fibrils gave the highest measured adhesion forces. The data suggest that a proper alignment of the fibrillar arrays could be achieved using a DL ratio between  $0$  and  $5$ .

In the measurements using the longer fibrils (heights of  $\sim 1 \mu\text{m}$ ), the cantilever starts the dragging movement after compressing the fibrillar arrays to the preset force. Most of the fibrils underneath the cantilever might be compressed into a folded structure at the initial stage of this measurement. The shear movement of the cantilever moves from this initial contact point, stretching the attached fibrils to an extended position. Fibrils will likely point in the same direction that the cantilever is moving. Fully extended fibrils would expose more of their surface area to potential contact with the cantilever, creating more contact area. Thus, higher adhesion forces would be measured during the subsequent cantilever pull-up. However, if the dragging distance is much greater than the average length of the fibrils, the result could be a stick–slip effect as reported in the literature.<sup>26</sup> The sudden release of the fibrils from the flat cantilever could cause an unstable interaction and, subsequently, a loss of the optimized contact points formed during the previous shear movement. In addition, the excessive dragging movement could also increase the likelihood of damage to the fibrils,<sup>27,28</sup> although no change was observed in these studies (see the Experimental Section for further details). In the case of the shorter fibrils (heights of  $\sim 0.1 \mu\text{m}$ ), the adhesion forces measured by the PP method are

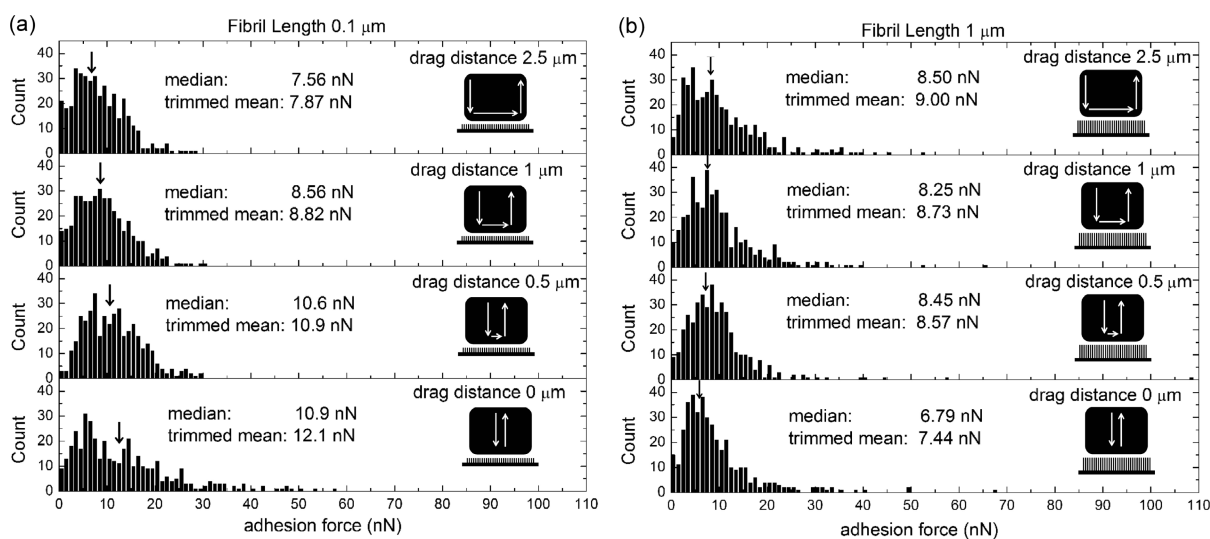


**Figure 4.** Histograms of adhesion forces measured by the LDP and PP methods for an array of (a) relatively short fibrils (average heights of  $\sim 0.1 \mu\text{m}$ ) and (b) longer fibrils (average heights of  $\sim 1 \mu\text{m}$ ) for different drag distances. Drag velocity was set at  $20 \mu\text{m/s}$  with a retract velocity of  $1 \mu\text{m/s}$ . Arrows above the histograms indicate the location of the medians for each set of data.

the result of contact of the cantilever with both the fibrils and the recesses of the substrate between the fibrils. After initiating the drag movement, the cantilever contacted other fibrils and reduced its contact with the recessed regions. A decrease in the measured adhesion force for these samples was observed (Figure 4a) in correlation to extensive dragging movement of the cantilever. A decrease in the average adhesion force could indicate a possible reduction of contact area between the sample and the tipless cantilever.

Significant variations were observed between the distributions within the data for measurements on the shorter fibrils (Figure 4a). The longer the drag distance, the narrower was the observed distribution in measured adhesion force. Although a lower average adhesion force was measured for a drag distance of  $2.5 \mu\text{m}$ , its narrower distribution suggests that the contact between the fibrils and the cantilever was more uniform between different measurements. In contrast, the measurements for the longer fibrils had a relatively wide distribution of adhesion forces and the average adhesion force increased in correlation with an increased drag distance. The distributions observed in the data for the longer fibrils (Figure 4b) each had a similar appearance for all drag distances. The data also indicates that any shear movement during the fibril-cantilever interactions will increase the measured adhesion force for these samples in comparison to the results obtained by the PP method. The effect of fibril alignment during the “drag” step is more obvious in the longer fibrils. The *p*-values of the Kruskal–Wallis ANOVA, a nonparametric test suitable for non-Gaussian distributions,<sup>29</sup> on data collected for each sample was significantly small ( $<0.01$ ) suggesting that the drag distance is significantly influencing the measured adhesion force. The influence of drag distance on the measured adhesion force revealed that the interactions between the flat cantilever and the fibrillar arrays are not as simple as predicted by classical friction laws and contact mechanics. Although these predictions are applicable in the case of PP based measurements, further description of the system is needed when using the LDP method. The dragging movement introduced variations in the measured adhesion force as seen in Figure 4. Changes to the interaction points between the contacting surfaces and, potentially, surface charging between these two materials could be the primary causes of the observed variation in adhesion forces. The experimental design for the LDP measurements included a 2 s dwell time after the dragging step and before the separation of the two contacting surfaces. This dwell time was incorporated to allow for the dissipation of surface charges (e.g., possibly from the sample to the reflective gold coating on the top surfaces of the cantilever). This dwell time was also incorporated to account for potential contributions from changes in the material properties of the fibrils during the dragging movement (e.g., stiffness, viscosity and/or viscoelasticity).<sup>30</sup> Therefore, the primary contributions to the observed increases or decreases in adhesion forces were attributed to the formation and loss of contact points between the two materials. Additional studies that varied the drag velocity were performed to further investigate the range of effects resulting from the lateral shear movements of the cantilever.

**2.2. Investigation of the Drag Velocity in LDP Experiments.** Velocity of the cantilever during the drag movement of the LDP measurements could be important for its influence on providing sufficient time to form a significant number of interactions between the contacting surfaces. Figure

5 depicts a typical FT curve of a LDP measurement on the  $\sim 0.1 \mu\text{m}$  tall fibrils. The magnified traces within the insets located

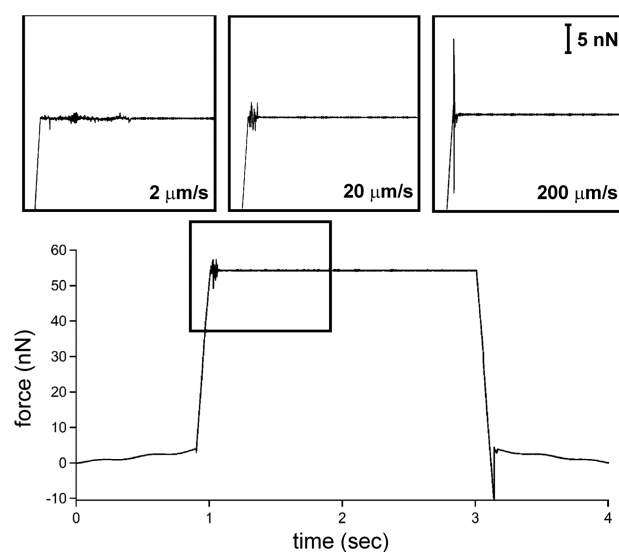


**Figure 5.** Typical force–time (FT) curve (bottom) measured using the LDP method for an array of  $0.1 \mu\text{m}$  tall fibrils. Drag distance was set at  $1 \mu\text{m}$ . The insets are magnified FT curves that depict the variation observed in these curves for different drag velocities (e.g., 2, 20, and  $200 \mu\text{m/s}$ ) using the LDP method. The oscillations in the measured force increased in proportion to the drag velocity (as noted in the insets) when the cantilever was in motion (i.e., the dragging step) while in contact with the fibrillar arrays. The magnitude of oscillations in the measured force varied from  $\sim 1$  to  $\sim 15 \text{ nN}$ .

above the FT curve depict the force response during the dragging process for different drag speeds. The magnitude of the variation in force observed during this dragging increased significantly with an increase in the speed of the lateral shear. The magnitudes of the observed oscillations in the measured forces at a drag speed of 2, 20, and  $200 \mu\text{m/s}$  were  $\sim 1$ ,  $\sim 5$ , and  $\sim 15 \text{ nN}$ , respectively. The duration of the drag can also be observed in these plots. In all cases, a 2 s dwell time was introduced after the drag movement in order to provide a sufficient amount of time for the system under study to relax and to maximize the interactions between the contacting surfaces prior to measuring the resulting adhesion forces.

The energy needed to overcome the maximum static friction of the sample is theoretically the same for the higher drag speed as that for the lower drag speed. Therefore, when the drag speed is increased (i.e., drag time decreases) the force response should increase proportionally based on the conservation of energy. A slower drag movement could, however, generate a higher measured adhesion force because of a longer interaction time between the two types of surfaces establishing more points of contact. This hypothetical situation is supported by results of the statistical analysis of the LDP measurements from samples having both longer ( $\sim 1 \mu\text{m}$ ) and shorter ( $\sim 0.1 \mu\text{m}$ ) fibrils. Histograms for the results of the LDP measurement on the shorter fibrils are plotted in Figure 6a. Although the differences in average adhesion force between the three different drag speeds are within 1 nN of each other, the slower drag speed had a slightly higher average adhesion force than the results of the faster drag speed. The variance in the data, from slower to faster drag, was 36.8, 31.5, and 28.4 nN. Levene’s test was used to indicate if equal variance existed between the groups of data<sup>29</sup>

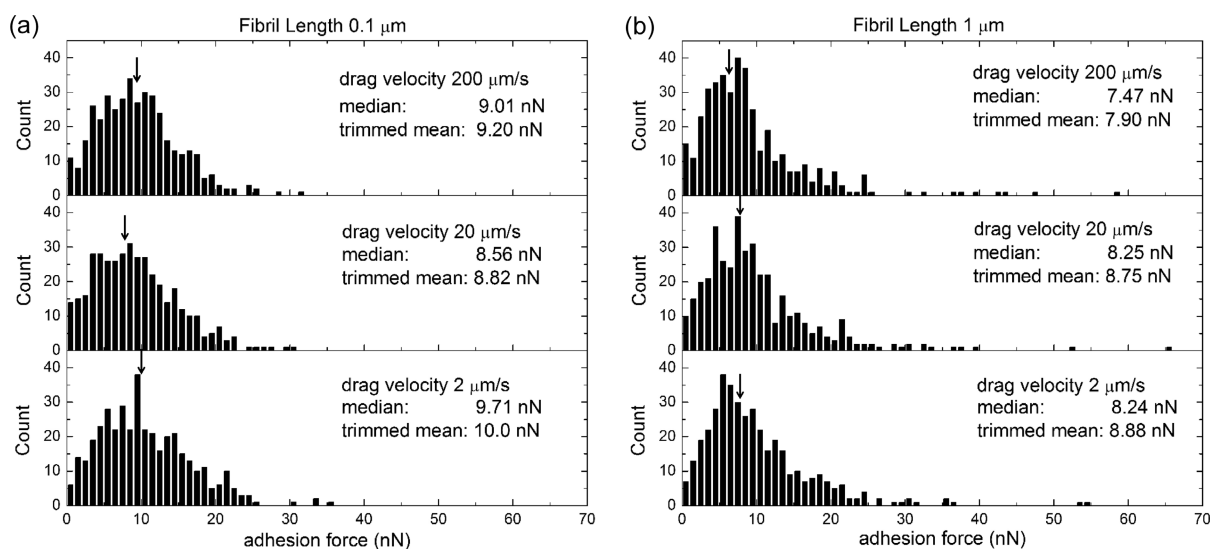


**Figure 6.** Histograms of the adhesion forces acquired by the LDP method for arrays of relatively (a) short fibrils (average heights of  $\sim 0.1 \mu\text{m}$ ), and (b) long fibrils (average heights of  $\sim 1 \mu\text{m}$ ) using different drag velocities (e.g., 2, 20, and  $200 \mu\text{m/s}$ ). Drag distance was set at  $1 \mu\text{m}$ . Arrows indicate location of medians for each set of data.

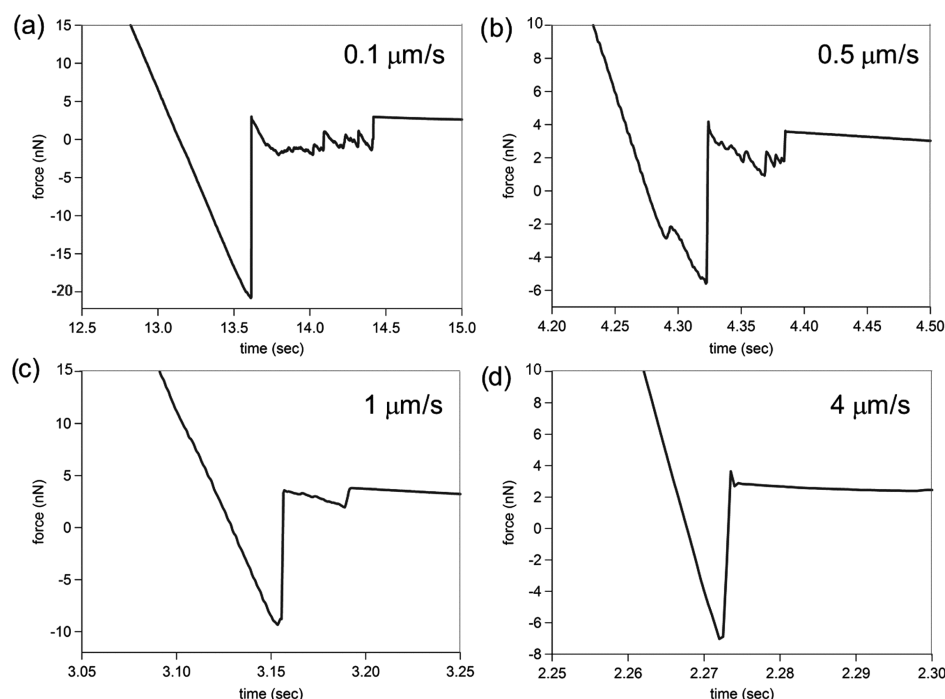


**Figure 7.** Representative force–time curves corresponding to different retract velocities, (a) 0.1, (b) 0.5, (c) 1, and (d)  $4 \mu\text{m/s}$ , following LDP-based measurements when separating the SPM controlled cantilever from an array of fibrils (average heights of  $\sim 0.1 \mu\text{m}$ ). The figures depict the portion of the FT curves upon reaching complete detachment of the cantilever from the fibrillar surfaces. Drag distance and velocity were set at  $1 \mu\text{m}$  and  $20 \mu\text{m/s}$ , respectively.

(see Experimental Section for further details). The  $p$ -value of Levene's test was 0.079, which indicated a small possibility for equal variance among these data sets. The lower variance in the data for the higher drag speed implies that the uniformity of the adhesion force is greater at fast lateral shear movements. The shape of each distribution was similar to each other. The decrease in average adhesion force in the faster drag experiments might also be the result of surface damage due to the high forces applied over a relatively short duration to overcome frictional forces. The rapid movement of the cantilever might also introduce more random points of contact

with the sample, such as slip between the fibrils and the flat cantilever. This tendency was more obvious in the experiments performed on the samples with longer fibrils (Figure 6b).

The average adhesion force decreases in proportion to an inverse in drag velocity in the measurements using longer fibrils. Differences between each of these sets of data were within 1 nN, but the variance in the data, from 2 to  $200 \mu\text{m/s}$ , was 49.7, 57.0, and 52.7 nN, respectively. These values were higher than the results obtained for the shorter fibrils. The  $p$ -value of the Levene's test is 0.845, showing a much higher tendency of equal variance among the data sets obtained for the

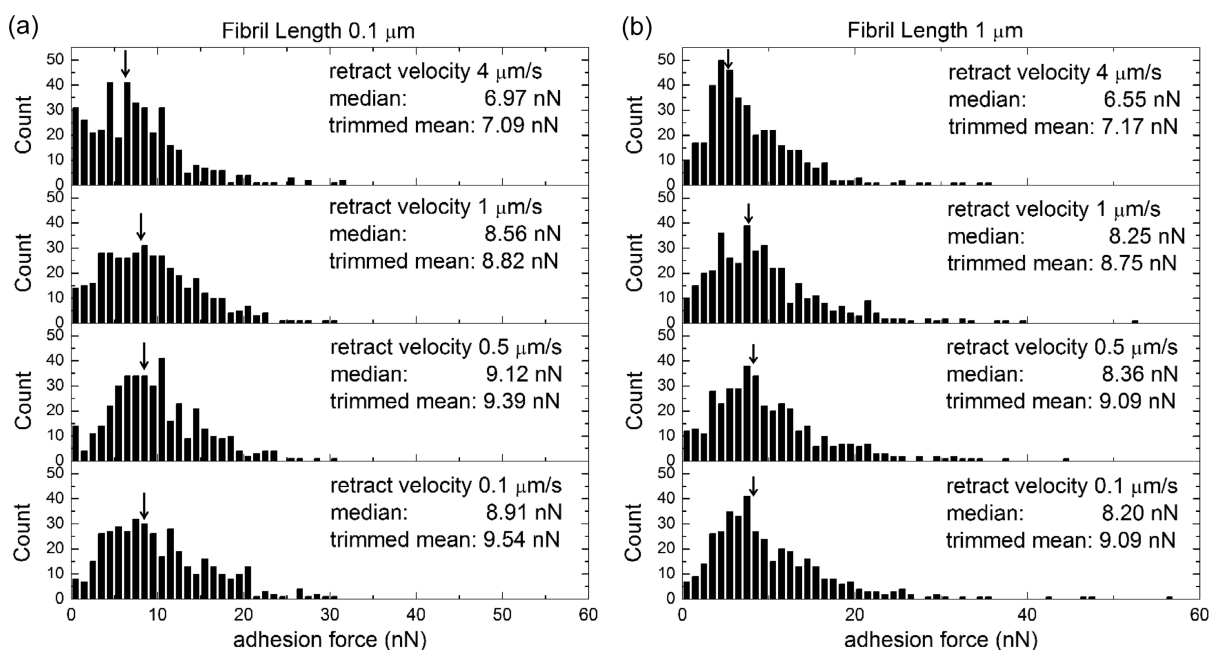


**Figure 8.** Histograms of adhesion forces acquired using the LDP method for (a) an array of  $\sim 0.1 \mu\text{m}$  tall fibrils and (b) an array of  $\sim 1 \mu\text{m}$  tall fibrils with different velocities for retraction of the SPM cantilever from these fibrillar surfaces. Drag distance and velocity were set at  $1 \mu\text{m}$  and  $20 \mu\text{m/s}$ , respectively. Arrows above each data set indicate the location of the median values for each sample.

longer fibrils in comparison to the shorter fibrils. The more equal the calculated variance in the data indicates that the test results were more consistent for the average adhesion force. In particular, the force distributions obtained at shear velocities of 20 and  $200 \mu\text{m/s}$  had very similar shapes. Despite the significant change in drag speed, the similar results obtained for these two sets of data implied that the interactions between the cantilever and the fibrils were similar, and that the possibility of fibril damage was very limited. The measured adhesion at the median and trimmed mean (both  $\sim 8 \text{ nN}$ ) for LDP measurements at  $20 \mu\text{m/s}$  drag velocity were coincident with the peak adhesion force in the histogram, suggesting a central tendency of the data set that matches the histogram shape. The other data sets in this particular study did not have the same property. The  $p$ -values of the Kruskal–Wallis ANOVA for the samples of shorter and longer fibrils were 0.013 and 0.042, respectively. This result indicated that drag velocity did not significantly influence the adhesion force in contrast to the results of varying the drag distance. The loading and dragging processes of the LDP method have been studied by varying drag distance and drag velocity. These studies revealed further insight into contact formation between the fibrils and the tipless cantilever. Disrupting the points of contact during the subsequent pulling movement was studied by also systematically investigating the vertical retraction of the cantilever from these fibrillar surfaces.

**2.3. Investigation of the Retract Velocity in LDP Experiments.** The process of retraction of the cantilever from the fibrillar surfaces contains important information on the release of the established contacts. Adhesion force recorded for each measurement was defined as the minimum force, or maximum attraction force, achieved during the cantilever retraction. The adhesion force though does not represent all aspects of the detachment process.<sup>3,8,23</sup> A series of typical measurements obtained using different pull up speeds for the cantilever, representing the portion of the FT curves that correlate with the period of cantilever retraction, were plotted

in Figure 7. All of these traces have a sharp peak at the period in time when the two contacting surfaces were completely separated. The peak force indicates that the cantilever was significantly bent right before the moment of separation. Significant oscillations were observed when the retract speeds were relatively slow. These oscillations might be the result of re-engaging interactions between the cantilever and the fibrils. After the sudden separation of the two types of surfaces, the thin cantilever itself would oscillate for a few cycles in resemblance to a springboard after unloading an applied force. The cantilever could further interact with the fibrillar surfaces during these cycles depending on the distance of retraction, which was directly proportional to the retract velocity. Some of the observed oscillations might, therefore, be attributed to further interactions between the cantilever and the arrays of fibrils during the retraction step. As the speed of retraction increased, the probability of this interaction decreased as observed in the data plots (Figure 7). These oscillations did not change the adhesion performance of the fibrillar samples.

Details of the detachment process were investigated by appropriately scaling the FT curves in Figure 7. The slope of the FT curve at the highest retract velocity was actually much steeper than it appears in this figure. A rapid retraction of the cantilever may cause perturbation to the established contacts even before a complete detachment. The influence of the retraction velocity can be more clearly observed in a statistical analysis of the adhesion forces for the arrays of shorter and longer fibrils (Figure 8). Both samples had a lower measured adhesion force for LDP measurements with a higher retract velocity.

In the measurements performed on the arrays of shorter fibrils (Figure 8a), the shape of the histogram for data obtained using a retract speed of  $1 \mu\text{m/s}$  most closely resembles a normal distribution. This histogram had a flat peak that closely corresponded to the median and trimmed mean. This result

suggests a high probability of measuring adhesion forces near the median and trimmed mean. The retract velocity of 0.5  $\mu\text{m/s}$  exhibited the best average adhesion among the four different velocities tested in these studies. The variance of adhesion (27.9 nN) measured using a 0.5  $\mu\text{m/s}$  retract velocity was the smallest in all of these measurements. The variance observed in the other sets of data, from lower to higher retract velocities, was 35.9, 31.5, and 45.2 nN. The *p*-value of Levene's test was 0.376, showing a relatively high possibility for equal variances. A retract velocity of 4  $\mu\text{m/s}$  had the lowest average adhesion and the most symmetric distribution of measured adhesion forces (Figure 8a) in comparison to the data sets obtained at the other retract velocities. These results indicated instability in the interactions between the cantilever and the fibrillar surfaces caused by the relatively quick withdrawal of the cantilever. It can be also concluded that a less predictable adhesion force can be expected when using a relatively high retract velocity. The overall Kruskal–Wallis *p*-value was  $\ll 0.01$ , further indicating that retract velocity significantly influences the adhesion force measured by the LDP method.

Similar trends were observed for the average adhesion forces measured for the longer fibrils and the shorter fibrils, but their histograms exhibited a significant difference in overall shape. The highest median and trimmed mean for the adhesion forces were observed for data obtained using a retract velocity of 0.5  $\mu\text{m/s}$ , but these results were similar to those obtained using retract velocities of 0.1 and 1  $\mu\text{m/s}$  (Figure 8b). The shapes of the histogram for these three sets of data were also a close resemblance of each other. The calculated variances of all four sets of data, from slow to fast retract velocities, were 53.8, 45.8, 57.0, and 30.1 nN, respectively. The *p*-value of Levene's test was 0.04, indicating a relatively different variance among the data sets. The variance and average adhesion force obtained using a retract velocity of 4  $\mu\text{m/s}$  drastically decreased in comparison to the other tests, suggesting a general degradation in adhesion performance using fast retraction speeds. The Kruskal–Wallis ANOVA *p*-value is  $\ll 0.01$ , which is a similar result to that obtained for the shorter fibrils. In summary, for measurements using different retract velocities a fast withdrawal (e.g., 4  $\mu\text{m/s}$ ) of the cantilever decreases the adhesion performance of both the shorter and longer fibrils. A retract velocity of 0.5  $\mu\text{m/s}$ , generally, provides the best adhesion performance for these samples. The retract velocity of the cantilever significantly influences the adhesion force measured using the LDP method.

### 3. CONCLUSION

Geckos have developed their own way to efficiently climb different surfaces. Observation on the movement of geckos inspired the development of a load–drag–pull measurement technique using a scanning probe microscope. The utility of the LDP method is to characterize the adhesive properties of materials and to provide further insight into an optimal set of parameters for using materials inspired by the nanosized fibrils on a gecko's foot. The lateral distance and velocity of the cantilever during the drag step, and the velocity at which the cantilever was pulled away from a surface were studied for their influence on the measured adhesion force of fibrillar samples. In this study, two samples were compared one with shorter ( $\sim 0.1 \mu\text{m}$ ) fibrils and another with longer ( $\sim 1 \mu\text{m}$ ) fibrils. A systematic study was performed on each parameter along with a detailed analysis of the information contained within the resulting force–time curves. A further statistical analysis was also

performed on the large sets of data collected using the LDP method on a SPM system. The relationship of the tested parameters to the measured adhesion force was not predicted by classical mechanics and friction theories. Observation on the force–time response of the LDP measurements revealed further details into the interactions between the flat cantilever and the fibrillar surfaces. The adhesion force measurements also revealed a difference in response to varying test parameters when comparing the results of samples with different fibril lengths. The drag velocity did not have as significant an influence on the measured adhesion force in comparison to changes in the drag distance and retract velocity. The drag distance had a greater influence on the results obtained for the longer fibrils than for the shorter ones, which was attributed to differences in fibril alignment and overall contact area with the tipless cantilever. Rapid cantilever withdrawal from the fibrillar surfaces generally reduced the measured adhesion forces. A moderate retraction velocity of the cantilever, specifically 0.5  $\mu\text{m/s}$ , provided the highest average adhesion from all the tested velocities in samples of both the longer and shorter fibrils. These results provided insight into the interactions between the cantilever and the fibrillar surfaces, and also guidance for future experiments on the gecko-like fibrillar adhesives. Applications, such as the use of fibrillar adhesives on climbing robots, will benefit from the results obtained from this study.

### ■ ASSOCIATED CONTENT

#### Supporting Information

Experimental section; estimation of contact area in the adhesion force instruments (PDF). This material is available free of charge via the Internet at <http://pubs.acs.org>.

### ■ AUTHOR INFORMATION

#### Corresponding Author

\*E-mail: [bgates@sfu.ca](mailto:bgates@sfu.ca).

#### Notes

The authors declare no competing financial interest.

### ■ ACKNOWLEDGMENTS

This work was supported in part by the Natural Sciences and Engineering Research Council (NSERC) of Canada, and the Canada Research Chairs Program (B.D. Gates). This work made use of 4D LABS shared facilities supported by the Canada Foundation for Innovation (CFI), British Columbia Knowledge Development Fund (BCKDF), Western Economic Diversification Canada, and Simon Fraser University. We appreciate the assistance of Jason Bemis at Asylum Research for assistance in codeveloping the software necessary for measuring adhesion forces resulting from shear induced alignment of fibrils using scanning probe microscopy techniques.

### ■ REFERENCES

- (1) Autumn, K.; Sitti, M.; Liang, Y. A.; Peattie, A. M.; Hansen, W. R.; Sponberg, S.; Kenny, T.; Fearing, R.; Israelachvili, J. N.; Full, R. J. Evidence for van der Waals Adhesion in Gecko Setae. *Proc. Natl. Acad. Sci. U.S.A.* **2002**, *99*, 12252–12256.
- (2) Autumn, K.; Majidi, C.; Groff, R. E.; Dittmore, A.; Fearing, R. Effective Elastic Modulus of Isolated Gecko Setal Arrays. *J. Exp. Biol.* **2006**, *209*, 3558–3568.
- (3) Tian, Y.; Pesika, N.; Zeng, H.; Rosenberg, K.; Zhao, B.; McGuiggan, P.; Autumn, K.; Israelachvili, J. Adhesion and Friction in Gecko Toe Attachment and Detachment. *Proc. Natl. Acad. Sci. U.S.A.* **2006**, *203*, 19320–19325.



- (4) Autumn, K.; Liang, Y.; Hsieh, T.; Zesch, W.; Chan, W.-P.; Kenny, T.; Fearing, R.; Full, R. J. Adhesive Force of a Single Gecko Foot-Hair. *Nature* **2000**, *405*, 681.
- (5) Li, Y.; Zhang, C.; Zhou, J. H.-W.; Menon, C.; Gates, B. D. Measuring Shear Induced Adhesion of Gecko-Inspired Fibrillar Arrays Using Scanning Probe Techniques. *Macromol. React. Eng.* **2013**, *7*, 638–645.
- (6) Autumn, K.; Dittmore, A.; Santos, D.; Spenko, M.; Cutkosky, M. Frictional Adhesion: a New Angle on Gecko Attachment. *J. Exp. Biol.* **2006**, *209*, 3569–3579.
- (7) Autumn, K.; Gravish, N. Gecko Adhesion: Evolutionary Nanotechnology. *Philos. Trans. R. Soc., A* **2008**, *366*, 1575–1579.
- (8) Gravish, N.; Wilkinson, M.; Autumn, K. Frictional and Elastic Energy in Gecko Adhesive Detachment. *J. R. Soc., Interface* **2008**, *5*, 339–348.
- (9) Murphy, M. P.; Aksak, B.; Sitti, M. Adhesion and Anisotropic Friction Enhancements of Angled Heterogeneous Micro-Fiber Arrays with Spherical and Spatula Tips. *J. Adhes. Sci. Technol.* **2007**, *21*, 1281–1296.
- (10) Schubert, B.; Lee, J.; Majidi, C.; Fearing, R. S. Sliding Induced Adhesion of Stiff Polymer Microfiber Arrays: 2. Microscale Behavior. *J. R. Soc., Interface* **2008**, *5*, 845–853.
- (11) Piccardo, M.; Chateauminois, A.; Fretigny, C.; Pugno, N. M.; Sitti, M. Contact Compliance Effects in the Frictional Response of Bioinspired Fibrillar Adhesives. *J. R. Soc., Interface* **2013**, *10*, 20130182.
- (12) Autumn, K.; Hsieh, S. T.; Dudek, D. M.; Chen, J.; Chitaphan, C.; Full, R. J. Dynamics of Geckos Running Vertically. *J. Exp. Biol.* **2006**, *209*, 260–272.
- (13) Lee, J.; Bush, B.; Maboudian, R.; Fearing, R. S. Gecko-Inspired Combined Lamellar and Nanofibrillar Array for Adhesion on Non-Planar Surface. *Langmuir* **2009**, *25*, 12449–12453.
- (14) Gorb, S.; Varenberg, M.; Peressadko, A.; Tuma, J. Biomimetic Mushroom-Shaped Fibrillar Adhesive Microstructure. *J. R. Soc., Interface* **2007**, *4*, 271–275.
- (15) Jeong, H. E.; Lee, J.-K.; Kim, H. N.; Moon, S. H.; Suh, K. Y. A Nontransferring Dry Adhesive with Hierarchical Polymer Nanohairs. *Proc. Natl. Acad. Sci. U.S.A.* **2009**, *106*, 5639–5644.
- (16) Menguc, Y.; Yang, S. Y.; Kim, S.; Rogers, J. A.; Sitti, M. Gecko-Inspired Controllable Adhesive Structures Applied to Micromanipulation. *Adv. Funct. Mater.* **2012**, *22*, 1246–1254.
- (17) Kim, S.; Spenko, M.; Trujillo, S.; Heyneman, B.; Santos, D.; Cutkosky, M. R. Smooth Vertical Surface Climbing with Directional Adhesion. *IEEE Trans. Robot.* **2008**, *24*, 65–74.
- (18) Mahdavi, A.; Ferreira, L.; Sundback, C.; Nichol, J. W.; Chan, E. P.; Carter, D. J. D.; Bettinger, C. J.; Patanavanich, S.; Chignozha, L.; Ben-Joseph, E.; Galakatos, A.; Pryor, H.; Pomerantseva, I.; Masiakos, P. T.; Faquin, W.; Zumbuehl, A.; Hong, S.; Borenstein, J.; Vacanti, J.; Langer, R.; Karp, J. M. A Biodegradable and Biocompatible Gecko-Inspired Tissue Adhesive. *Proc. Natl. Acad. Sci. U.S.A.* **2008**, *105*, 2307–2312.
- (19) Yang, S. Y.; Carlson, A.; Cheng, H.; Yu, Q.; Ahmed, N.; Wu, J.; Kim, S.; Sitti, M.; Ferreira, P. M.; Huang, Y.; Rogers, J. A. Elastomer Surfaces with Directionally Dependent Adhesion Strength and Their Use in Transfer Printing with Continuous Roll-to-Roll Applications. *Adv. Mater.* **2012**, *24*, 2117–2122.
- (20) Kim, Y.; Claus, R. K.; Limanto, F.; Fearing, R. S.; Maboudian, R. Friction Characteristics of Polymeric Nanofiber Arrays against Substrates with Tailored Geometry. *Langmuir* **2013**, *29*, 8395–8401.
- (21) Izadi, H.; Golmakani, M.; Penlidis, A. Enhanced Adhesion and Friction by Electrostatic Interactions of Double-Level Teflon Nanopillars. *Soft Matter* **2013**, *9*, 1985–1996.
- (22) Hu, S.; Xia, Z.; Gao, X. Strong Adhesion and Friction Coupling in Hierarchical Carbon Nanotube Arrays for Dry Adhesive Applications. *ACS Appl. Mater. Interfaces* **2012**, *4*, 1972–1980.
- (23) Gravish, N.; Wilkinson, M.; Sponberg, S.; Parness, A.; Esparza, N.; Soto, D.; Yamaguchi, T.; Broide, M.; Cutkosky, M.; Creton, C.; Autumn, K. Rate-Dependent Frictional Adhesion in Natural and Synthetic Gecko Setae. *J. R. Soc., Interface* **2009**, *7*, 259–269.
- (24) Puthoff, J. B.; Holbrook, M.; Wilkinson, M. J.; Jin, K.; Pesika, N. S.; Autumn, K. Dynamic Friction in Natural and Synthetic Gecko Setal Arrays. *Soft Matter* **2013**, *9*, 4855–4863.
- (25) Zhang, C.; Zhou, J. H.-W.; Sameoto, D.; Zhang, X.; Li, Y.; Ng, H. W.; Menon, C.; Gates, B. D. Determining Adhesion of Nonuniform Arrays of Fibrils. *J. Adhes. Sci. Technol.* **2014**, *28*, 320–336.
- (26) Das, S.; Chary, S.; Yu, J.; Tamelier, J.; Turner, K. L.; Israelachvili, J. N. JKR Theory for the Stick-Slip Peeling and Adhesion Hysteresis of Gecko Mimetic Patterned Surfaces with a Smooth Glass Surface. *Langmuir* **2013**, *29*, 15006–15012.
- (27) Lee, D. H.; Kim, Y.; Fearing, R. S.; Maboudian, R. Effect of Fiber Geometry on Macroscale Friction of Ordered Low-Density Polyethylene Nanofiber Arrays. *Langmuir* **2011**, *27*, 11008–11016.
- (28) Gillies, A. G.; Fearing, R. S. Shear Adhesion Strength of Thermoplastic Gecko-Inspired Synthetic Adhesive Exceeds Material Limits. *Langmuir* **2011**, *27*, 11278–11281.
- (29) Montgomery, D. C. *Design and Analysis of Experiments*, 8th ed.; Wiley: Hoboken, NJ, 2013.
- (30) Meyers, M. A.; Chawla, K. K. *Mechanical Behavior of Materials*, 2nd ed.; Cambridge University Press: Cambridge, U.K., 2008.